Finite Element Study of Implant Subsidence and Medial Tilt in Agility Ankle Replacement

Authors' Contribution:
Study Design A
Data Collection B
Statistical Analysis C
Data Interpretation D
Manuscript Preparation E
Literature Search F
Funds Collection G

BCE Yunwei Cui*
BC Pan Hu*
CDE Ning Wei*
CDF Xiaodong Cheng
DF Wenli Chang
A Wei Chen

Department of Orthopedic Surgery, The Third Hospital of Hebei Medical University, Orthopedic Research Institution of Hebei Province, Key Laboratory of Biomechanics of Hebei Province, Shijiazhuang, Hebei, P.R. China

Corresponding Author:
Source of support:

* These authors contributed equally to this work
Wei Chen, e-mail: surgeonchenwei@126.com
Hebei National Science Foundation-Outstanding Yonth Foundation (Grand No. H 2017206104)

Background: Clinical studies indicate that in total ankle arthroplasty, postoperative implant subsidence and medial tilt become two significant concerns of the ankle replacement system, and which are associated with the contact between the bones and the talar component. Up to now, little attention has focused on the contact between the bones and the talar component.

Material/Methods: In order to address implant subsidence and medial tilt, one three-dimensional finite element model of contact between the bone and the talar components was built with the material properties of the cancellous bone interpolated from the experimental data, which represents variation of material properties through the cancellous bones. The finite element model was used to study the following: variation of the Young's modulus of the bones, stiffness of the talar component, loading direction, and loading magnitude with the implant subsidence.

Results: The computational results reveal that a variety of Young's modulus of the cancellous bones causes the medial tilting of the talar component and that big plastic strains are associated with tilting. The implant subsidence increases from 0.169 mm to 0.269 mm when the loading changes from 272 kg to 408 kg. However, to the contrary, the implant subsidence decreases from 0.2676 mm to 0.1783 mm when Young's modulus of the bones increases 50%. However, the implant subsidence shows little change with a different Young's modulus of the talar component from 88 GPa to 132 GPa.

Conclusions: Our study indicates that a variety of different Young's modulus of the cancellous bones cause the medial tilting of the talar component. To solve subsidence and tilting, both the contact area and the variation of material properties should be taken into account.

MeSH Keywords: Ankle Fractures • Ankle Joint • Finite Element Analysis

Full-text PDF: https://www.medscimonit.com/abstract/index/idArt/906151

📄 2422   📊 4   📈 9   📚 21

Background

Total ankle replacement was introduced in the 1970s to restore normal ankle kinematics and kinetics [1]. In the last three decades, total ankle replacement has progressed considerably. Many modern total ankle replacement designs have been developed and generally are classified into two groups based on design: two-component and three-component (mobile-bearing) designs. The FDA approved the Agility (Depuy, Warsaw, Indiana) Total Ankle Replacement System, a two-component design, in 1992 [2]. It has undergone four generations and seven phases of improvement [3], and is widely used across the world, especially in the United States [1,3–7]. However, clinical studies have demonstrated that in total ankle arthroplasty, postoperative implant subsidence and medial tilt have emerge as two significant concerns of this system due to pain and ankle instability [8–11]. These concerns are related to the contact between the bones and the talar component. A few studies have explored contact stresses in the polyethylene (PE) liner [8–11], but little attention has focused on the contact between the bones and the talar component. This study analyzed contact between the bones and the talar component by using the finite element method with the variation of material properties through the bones. The computational results offer a better understanding of posterior subsidence and medial tilt, and provide a base for the new design of the ankle replacement.

Material and Methods

Geometry

The tibio-talar joint is composed of the tibia, fibula, ankle joint, and talus. This study addressed the implant subsidence. Therefore, the model, which is composed of the bones, talar component, and simplified PE liner for loading, focuses on the contact between the bones and the talar components. A talus from a 60-year-old female was scanned using MDCT on a 256-row MDCT Scanner (iCT, Philips, Netherlands; real spatial resolution: 230×230 µm; slice thickness: 0.67 mm) and digitized. Its geometry was built in MIMICS 10.0. Following the surgical guidelines, two thirds of the lateral and medial malleolae were left untouched, and the rest was cut for the tibial component. The corresponding geometry of the bone was modified in ANSYS17.0 workbench. After the geometry of the talar component was imported into the ANSYS workbench, the talar component, one part of the size 4 of AGILITY Ankle implant (DePuy Orthopaedics, Inc., a J&J Co., Warsaw, IN, USA), was positioned on the bones under the directions suggested by the surgical guidelines that the tibial component should be "flush both anteriorly and posteriorly". We simulated in-growth of the bones into the implant. This recess was cut by Boolean operations in ANSYS with the implant, allowing the interface
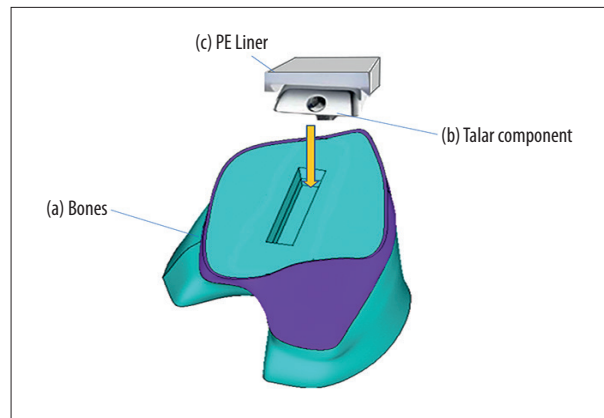

Figure 1. The Agility Total Ankle Replacement Model: a) bones; b) talar component; c) PE liner.

between the bone and implant as fully bonded. Then, a PE liner was placed on the top of the talar component (Figure 1). In the model, the contact between the bones and the implant was assumed to be perfectly bonded, while the contact between the PE liner and the talar component was regarded as standard contact.

Material properties

The Young's modulus of the talar component and PE were defined with 193 GPa and 577 MPa, respectively [8]. The bone included both cortical bone and cancellous bone, where a thin layer of the cortical bone covers the surface of the talus with a modulus of 17.6 GPa [12].

Clinical studies have demonstrated that bone, especially cancellous bone, is nonhomogeneous [13]. In order to take into account the cancellous bone, it is common to obtain the bone properties from the CT data [14–16]. However, this method is limited by the noise of the CT image and the empirical relation between the bone properties and CT data. In this study, we explored ways to apply multidimensional interpolation on nonhomogeneous cancellous bone with available experimental data. Jensen et al. [17] measured the Young's modulus of cancellous bones at the contact area, with twelve points for one layer and a total of three layers through the talus (Figure 2). Thus, they obtained Young's modulus of thirty-six different locations throughout the cancellous bones. With these experimental data, radial-basis interpolation, a global method, was selected to interpolate the material properties of the cancellous bones [18]. After the interpolation was completed in ANSYS 17.0, we obtained the material properties of cancellous bones that vary throughout the talus, as shown in Figure 3. In addition to the contact area, the cancellous bones in other areas were assigned with Young's modulus 280 Mpa [8] (Figure 4). Furthermore, the investigated talar bone was supposed to be loaded dominantly in compression; previous experiments [19]
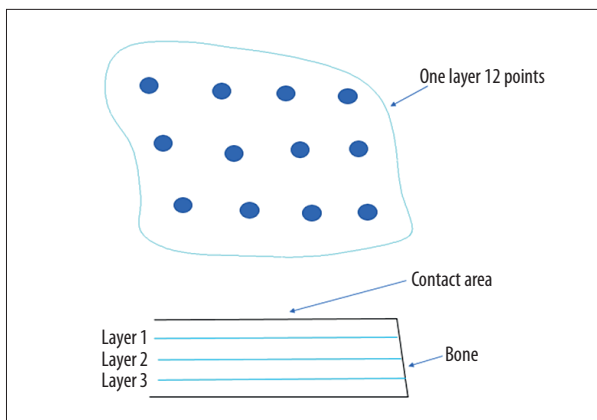
Figure 2. Schematic of Jensen's experiment [6]. The Young's modulus of cancellous bones was measured with one layer twelve points and a total of three layers through the talus depth.
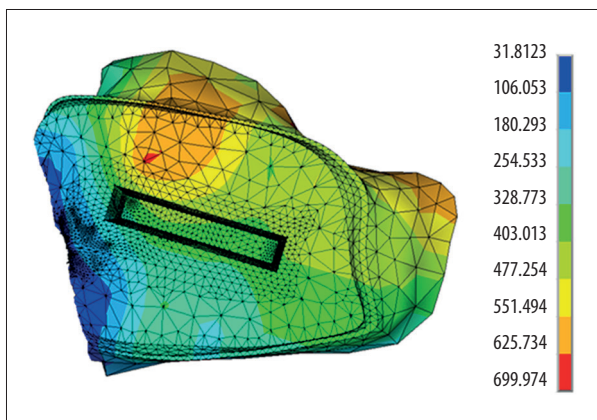

Figure 3. Variety of the material properties of the bone at the contact area (units in the Figure=MPa).

found that in compression, cancellous bone yields at strains around 1% and fails at around 2%. Therefore, the cancellous bones are simplified as perfect material with a yield strain at 1.5% in the FE model.

The Poisson's ratio of bones and the implant was assigned 0.3 [12].

Loading and boundary conditions

It is very difficult to determine forces transmitted across the ankle joint because this joint includes forces external and internal to the body. This study applied five times the body weight to the surface of the talar component [20]. A body weight of 68 kg was assumed here, so the total applied load was 340 kg. Our study also loaded in three different directions: plantar flexion (–20°), neutral flexion (0°), and dorsi flexion (+20°) (Figure 5). Plantar flexion (–20°) and dorsi flexion (+20°) are the range of pain-free ankle for normal daily activities after an ideal ankle
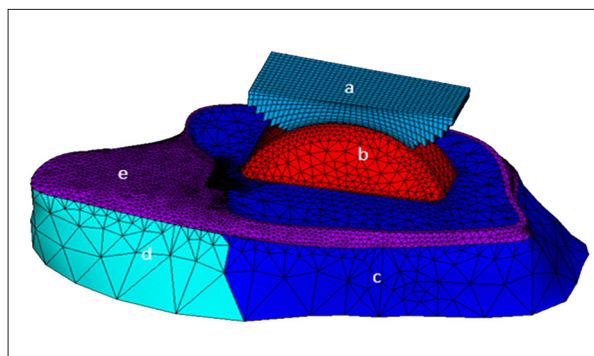

Figure 4. Finite element model of Agility Ankle Replacement (neutral flexion 0°): a) PE liner; b) talar component; c) cancellous bone interpolated from experimental data; d) cancellous bone with E=280 Mpa; e) cortical bone.
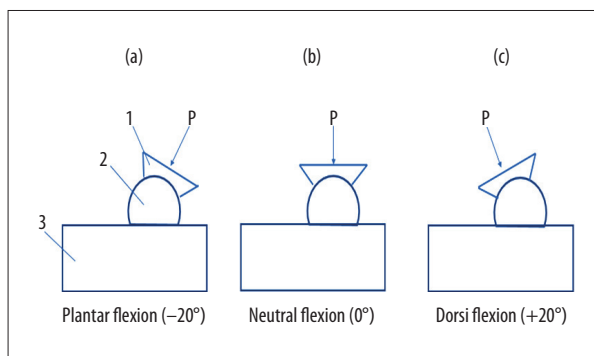

Figure 5. Schematic of loadings showing the plantar flexed, neutral, and dorsiflexed cases (P=3332N) (1 – Liner; 2 – talar component; 3 – talus). a) Plantar flexion (–20°); b) neutral flexion (0°); c) dorsi flexion (+20°).

arthroplasty [21]. The bottom surface of the talus was fixed in all six degrees of freedom.

Mesh and contact definition

The talus and the talar component were meshed with ten node tetrahedral elements, and the PE liner was meshed with eight node brick elements. The contact between the talar component and PE was defined as a standard contact with a coefficient of friction 0.07 in ANSYS for the PE liner slides on the talar component. Since bones grow to bond the talus to the implant, the bone-implant interface was modeled as perfectly bonded for simplification. The model consisted of more than 70,000 elements and 120,000 nodes (Figure 4). Its computation required about one hour with a 2.5 GHz Pentium 4 computer.

To verify the meshing sensitivity of the finite element model, a mesh refinement was conducted at the bone-implant interface where contact occurs. After doubling the mesh density, the change of the maximum von Mises (vM) stresses was

less than 2%. Therefore, the convergence of the finite element model was validated.

Results

The nodal displacements and the associated elemental vM stresses, as well as the elemental vM plastic strains in the bone when the forces are loaded in the different directions, appear in Figures 6–8, respectively. For a comparison, the cancellous bone was modified as a uniform Young's modulus 280 MPa [8]. Figure 9A–9C present the corresponding results.

Figures 6B, 7B, and 8B reveal that the big stresses occurred at the edge of the talar component, where the bone reaches plasticity and its stresses are equal to the yield stress. The maximum stresses in these three cases are located at the lateral edge and the posterior edge with the big Young's modulus (Figure 3), although the deformations of these locations are smaller than those along the medial edge. The maximum stresses in these three cases are very close, from 9.69 Mpa to 10.54 Mpa, much bigger than the maximum stress 7.52 Mpa of the comparison case with a uniform Young's modulus (Figure 9B). This indicates that the model with a uniform Young's modulus of the cancellous bones underestimates the maximum stress of the bones.

Mechanical strains are composed of elastic and plastic strains. Elastic strains recover after the external forces are removed, but plastic strains become permanent even with the absence of the external forces. Figures 6C, 7C, and 8C illustrate that the plastic strains occur mainly around the posterior edges and small regions along the medial edge with maximum plastic strain from 0.098 to 0.137. However, with a uniform Young's modulus, cancellous bones have plasticity only in the posterior with maximum plastic strain 0.101 (Figure 9C).

Parametric analysis was conducted to study the implant subsidence with the Young's modulus of the bones, Young's modulus of the talar component, loading direction, and loading magnitude. The base model was selected with dorsi flexion (0°), loading 340 kg and material properties defined in Section 'Material properties'. The results, which are listed in Tables 1–4, clearly show that the implant subsidence increases with the higher loading, lowers Young's modulus, and changes with different loading directions, but differs little with the different Young's modulus of the talar component.

Discussions

A three-dimensional finite element model of Agility Total Ankle was built with the material properties of the cancellous bones
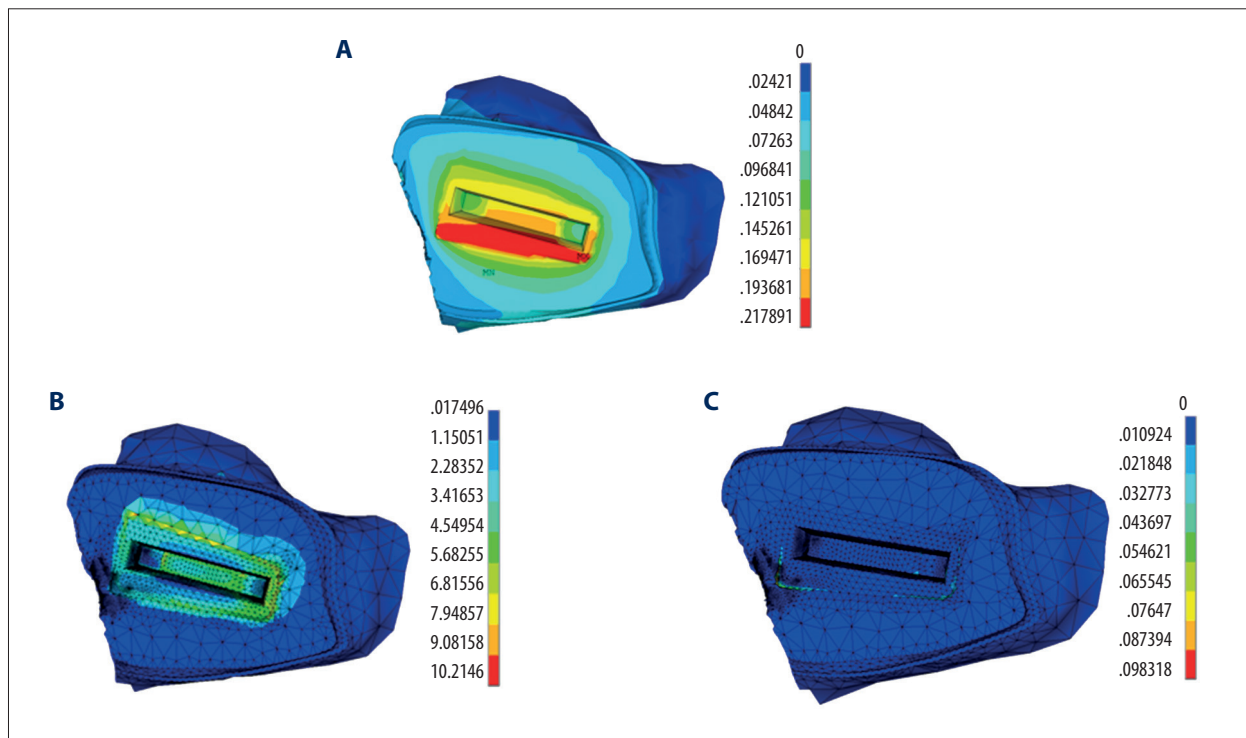

Figure 6. Computational results of the cancellous bones at the contact area in the plantar flexed case: (**A**) nodal deformation; (**B**) Von Mises stresses (Mpa); (**C**) Von Mises plastic strains.

Figure 7. Computational results of the cancellous bones at the contact area in the neutral case: (**A**) nodal deformation (tilting angle: 0.17°); (**B**) Von Mises stresses (Mpa); (**C**) Von Mises plastic strains.
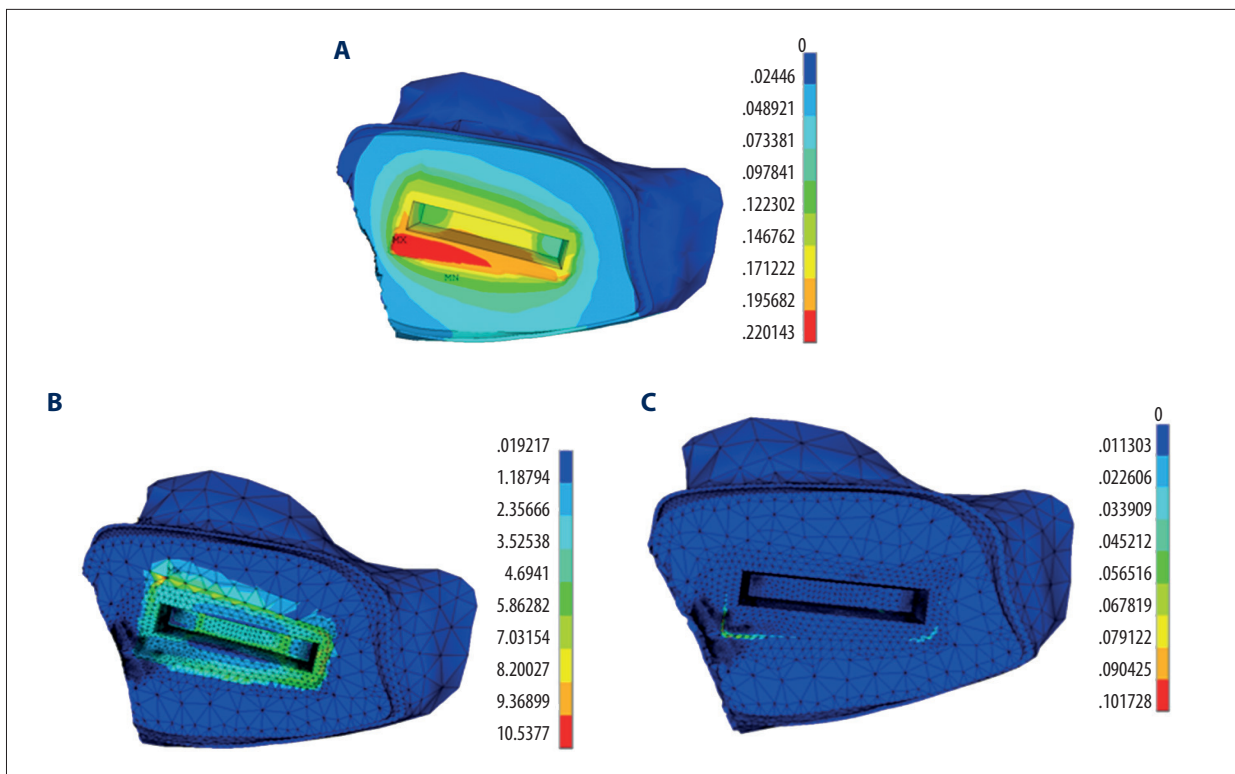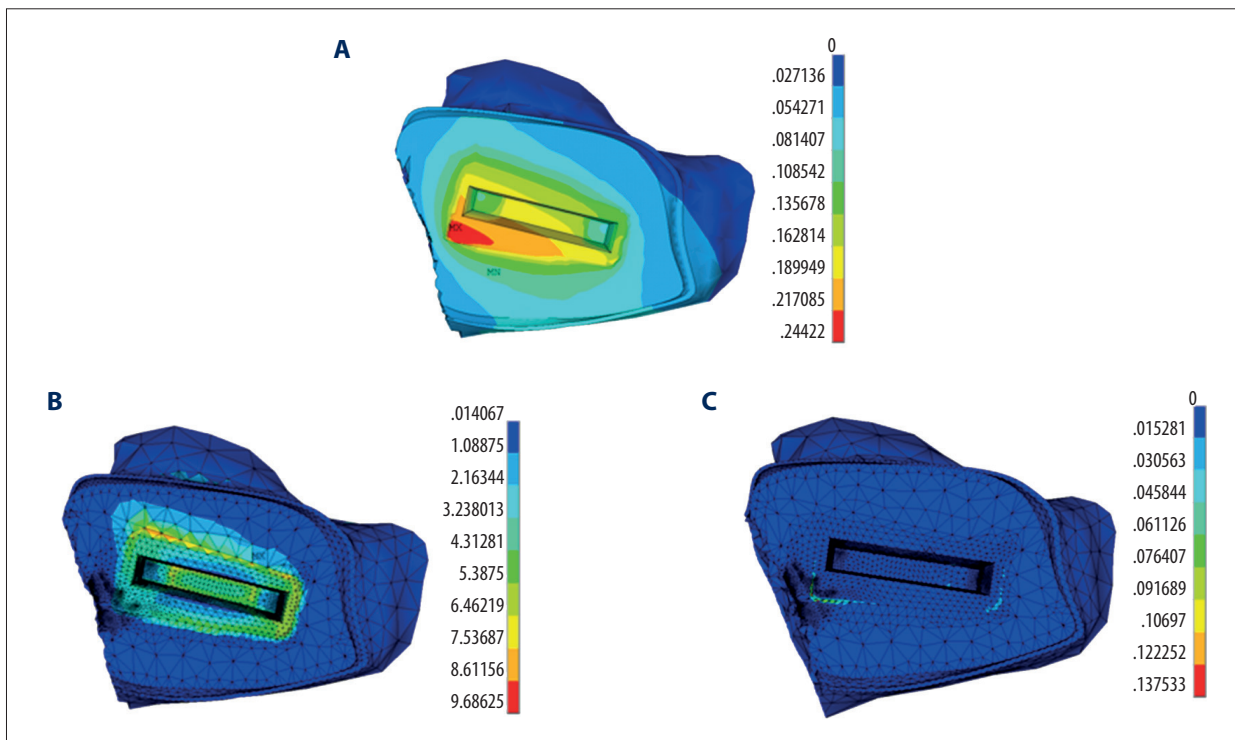

Figure 8. Computational results of the cancellous bones at the contact area in the dorsiflexed case: (**A**) nodal deformation (tilting angle: 0.20°); (**B**) Von Mises stresses (Mpa); (**C**) Von Mises plastic strains.
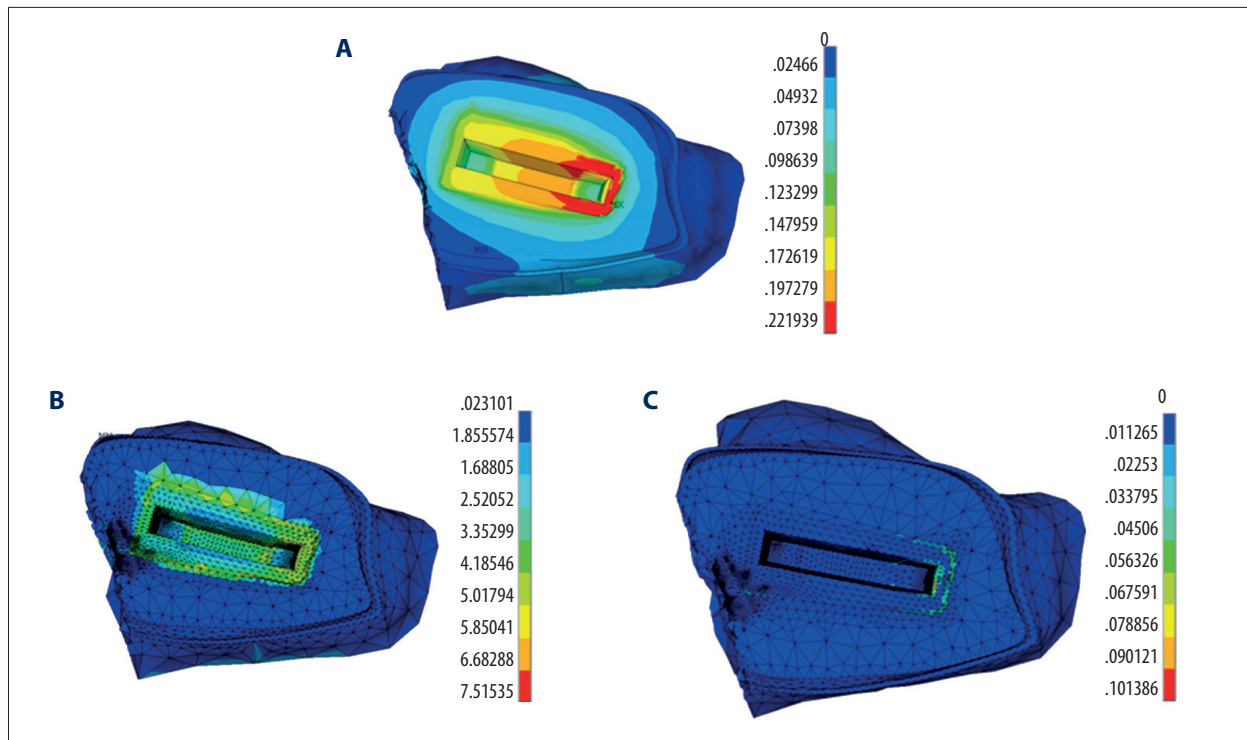
Figure 9. Computational results of the cancellous bones at the contact area with uniform Young's modulus in the neutral case: (**A**) nodal deformation (tilting angle: 0.33°); (**B**) Von Mises stresses (Mpa); (**C**) Von Mises plastic strains.

Table 1. Variation of the loading direction with the implant subsidence.

Dorsi flexion (°)	−20	0	20
Subsidence (mm)	0.217	0.220	0.244

Table 2. Variation of the loading magnitude with the implant subsidence.

Loading (kg)	272	340	408
Subsidence (mm)	0.169	0.220	0.269

Table 3. Variation of Young's modulus of the cancellous bones with the implant subsidence.

E scale factor	0.8	1.0	1.2
Subsidence (mm)	0.2676	0.220	0.1783

Table 4. Variation of Young's modulus of the talar component with the implant subsidence.

Young's modulus (GPa)	88	110	132
Subsidence (mm)	0.220	0.220	0.221

1129

Indexed in: [Current Contents/Clinical Medicine] [SCI Expanded] [ISI Alerting System] [ISI Journals Master List] [Index Medicus/MEDLINE] [EMBASE/Excerpta Medica] [Chemical Abstracts/CAS]

in the talus interpolated from the experimental data to represent the variation of material properties across the talus. The model included a realistic representation of structures as well as the loading conditions. The convergence of the finite element model was validated. The computational results of this model can be utilized to convincingly analyze the design of Agility Total Ankle.

The medial tilting of the component occurred at the locations where the Young's modulus is the smallest in the contact area. The contact between the talar component and the cancellous bones with various Young's modulus can be considered as the loaded talar component supported by a series of springs with different degrees of stiffness. The more compliant piece of the bone refers to the spring with the lower stiffness, which corresponds to the large deformation. Therefore, the talar component tilts from the bone part with the larger Young's modulus to that with the lower Young's modulus. On the contrary, with the uniform Young's modulus, the same stiffness should have the same deformation. Thus, little tilting occurs. Furthermore, the medial tilting changes with different loading directions. The tilting angle is 0.20° in the neutral flexion. It increases to 0.33° in the dorsi flexion in which the loading shifts closer to the area with the lower stiffness, and decreases to 0.17° in the plantar flexion in which the loading turns further from it.

The plastic strains occur mainly around the posterior edges and small regions along the medial edge. The reason for the posterior is due to its narrow contact area. The big plasticity at the medial edge results from the large deformation there. Because the cancellous bone was assumed to be a perfect plastic material, the plasticity is always associated with the bone's large deformation. Thus, the largest plasticity always occurs at the same location of the largest deformation in the tilting area. It is interesting to note that with a uniform Young's modulus, cancellous bones have plasticity only in the posterior. This suggests a connection between tilting and a large plasticity of the bones.

As aforementioned, the contact between the talar component and the bones can be simplified as the loaded talar component supported by springs. Thus, with the higher loading and lower Young's modulus of the bones, the implant subsidence increases. Also, the simplified spring model does not involve the properties of the talar component, which is why the implant subsidence changes little with the variety of the Young's modulus of the talar component. One approach for solving the subsidence issue is to increase the contact area between the bones and the talar component. This method makes sense because under the same loading with the larger contact area, the deformation and average stress of the bones become smaller. Therefore, the subsidence alleviates. However, the variation of the material properties of cancellous bones within the contact

area causes the tilting. An increase of the current contact area would make the difference between the largest Young's modulus and the smallest Young's modulus of the cancellous bones within the contact area a larger one, thereby worsening the tilting. As discussed above, because a worse tilting causes bigger plasticity, an increase of the current contact area would not necessarily solve the subsidence issue. The future design of the ankle replacement should take both the contact area and the variation of material properties into account.

In the traditional ankle replacement model, the cancellous model was designed with a uniform Young's modulus [8]. One significant feature of the current model is that the Young's modulus of the cancellous bones in the contact area was interpolated by the experimental data. With this feature, the computational results indicate that the tilting was observed in the deformation of the bones, compared to little tilting by the traditional model with a uniform Young's modulus of the cancellous bones. In addition, the maximum stresses by the current model are much higher than those caused by the traditional model, which means the traditional model underestimates the maximum stresses. Furthermore, the plastic strains in the current model occur primarily around the posterior edges and small regions along the medial edge, but the plastic strains appear only around the posterior edges in the traditional model. These differences indicate that it is necessary to build the ankle replacement model with the true cancellous bone material properties.

This study has many limitations. It had a little sample size. Also, the finite element model was not validated by the experimental data, although meshing sensitivity was studied to validate the convergence of the finite element model. In addition, the interface between the bone and the implant, assumed as fully bonded in the model, is an ideal connection and has no supporting evidence to support it. This limitation may affect our computational results. However, it does not affect the major conclusions of this study because the subsidence is the deformation of the cancellous bone and the medial tilting is due to the various material properties of the cancellous bone.

Conclusions

A three-dimensional finite element model of Agility Total Ankle was developed with the material properties of the cancellous bones in the talus interpolated from the experimental data. The computational results show that a variety of Young's modulus of the cancellous bones causes the medial tilting of the component. With the higher loading and lower Young's modulus of the bones, the implant subsidence increases. However, the implant subsidence changes little with a different Young's modulus of the talar component.

To reduce the medial tilting, the contact area between the talar component and the bones should be selected with less variation of the Young's modulus. In addition, we found that the largest plasticity occurred at the tilting area. Large plasticity and tilting were connected.

Conflicts of interest

None.

References:

1. Cerrato R, Myerson M: Total ankle replacement: The Agility LP prosthesis. Foot Ankle Clin, 2008; 13(3): 485–94

2. Gougoulias NE, Khanna A, Maffulli N: History and evolution in total ankle arthroplasty. Br Med Bull, 2009; 89(1): 111–51

3. Ellington JK, Gupta S, Myerson MS: Management of failures of total ankle replacement with the agility total ankle arthroplasty. J Bone Joint Surg Am, 2013; 95(23): 2112–18

4. Alvine GF, Alvine FG: Total ankle arthroplasty using the agility stemmed talar revisional component: Three to eight year follow-up. SD Med, 2016; 69(4): 151–54

5. Roukis TS, Simonson DC: Incidence of complications during initial experience with revision of the agility and agility lp total ankle replacement systems: A single surgeon's learning curve experience. Clin Podiatr Med Surg, 2015; 32(4): 569–93

6. Claridge RJ, Sagherian BH: Intermediate term outcome of the agility (TM) total ankle arthroplasty. Foot Ankle Int, 2009; 30(9): 824–35

7. Gougoulias N, Khanna A, Mcbride DJ, Maffulli N: Erratum to: How successful are current ankle replacements?: A systematic review of the literature. Clin Orthop Relat Res, 2010; 468(4): 199–208

8. Miller MC, Smolinski P, Conti S, Galik K: Stresses in polyethylene liners in a semiconstrained ankle prosthesis. J Biomecha Eng, 2004; 126(5): 636–40

9. Byrne N, Ploeg HL, Deffenbaugh D: Finite element analysis of a total ankle arthroplasty over one stance phase. ISB XXth Congress – ASB 29th Annual Meeting, July 31 – August 5, Cleveland, Ohio, 2005; 165

10. Espinosa N, Walti MP, Snedeker JG: Misalignment of total ankle components can induce high joint contact pressures. J Bone Joint Surg, 2010; 92(5): 1179–87

11. Elliott BJ: Optimization of WSU total ankle replacement systems. 2012

12. Rho JY, Kuhn-Spearing L, Zioupos P: Mechanical properties and the hierarchical structure of bone. Med Eng Phys, 1998, 20(2): 92–102

13. Pal S: Design of artificial human joints & organs. Springer US; 2014

14. Rho JY, Hobatho MC, Ashman RB: Relations of mechanical properties to density and CT numbers in human bone. Med Eng Phys, 1995; 17(5): 347–55

15. Carter DR, Hayes WC: The compressive behavior of bone as a two-phase porous structure. J Bone Joint Surg Am, 1977; 59(7): 954–62

16. Wirtz D, Schiffers NT, Radermacher K et al: Critical evaluation of known bone material properties to realize anisotropic FE-simulation of the proximal femur. J Biomech, 2000; 33(10): 1325–30

17. Jensen NC, Hvid I, Krøner K: Strength pattern of cancellous bone at the ankle joint. Eng Med, 1988; 17(2): 71–76

18. Amidror I, Amidror I: Scattered data interpolation methods for electronic imaging systems: A survey. Journal of Electronic Imaging, 2012; 11(2): 157–76

19. Kopperdahl DL, Keaveny TM: Yield strain behavior of trabecular bone. J Biomech, 1998; 31(7): 601–8

20. Stauffer RN, Chao EY, Brewster RC: Force and motion analysis of the normal, diseased, and prosthetic ankle joint. Clin Orthop Relat Res, 1977; 127(127): 189–96

21. Conti, SF, Wong YS: Complications of total ankle replacement. Clin Orthop Relat Res, 2001; 391: 105–14